

# Biodegradable Amphiphilic Copolymers Based on Poly( $\epsilon$ -caprolactone)-Graft Chondroitin Sulfate as Drug Carriers

Ai-Ling Chen,<sup>†</sup> Hsiao-Chen Ni,<sup>†</sup> Li-Fang Wang,<sup>\*,†</sup> and Jenn-Shing Chen<sup>‡</sup>

Faculty of Medicinal and Applied Chemistry, School of Life Science, Kaohsiung Medical University, Kaohsiung City 80708, Taiwan, and Department of Applied Chemistry, National University of Kaohsiung, Kaohsiung City 80811, Taiwan

Received May 1, 2008; Revised Manuscript Received June 25, 2008

The goal of this study was to develop a new type of core–shell micelles based on biocompatible and biodegradable amphiphilic copolymers, named PCL-CS, using chondroitin sulfate (CS) as a hydrophilic segment and poly( $\epsilon$ -caprolactone) (PCL) as a hydrophobic segment. The copolymers, prepared from the various compositions between CS and PCL, were characterized by Fourier transform infrared spectrometer, proton nuclear magnetic resonance spectrometer, and differential scanning calorimeter. The PCL-CS copolymers could be assembled into micelles using a simple emulsion. With the fluorescent probe technique, the critical micelle concentrations were obtained in the range of  $1.26 \times 10^{-3}$ – $8.86 \times 10^{-3}$  mg/mL. The spherical images of micelles were visualized in the presence of polyvinyl alcohol (PVA) with the use of the transmission electron microscope. The particle sizes of micelles were all smaller than 300 nm, neither aggregate nor change in hydrodynamic sizes after 15 days staying in solutions containing salts or PVA by dynamic light scattering. The intracellular uptake of KB cells incubated with PCL-CS micelles was evidenced by confocal laser scanning microscope upon loading fluorescein isothiocyanate labeled bovine serum albumin as a probe.

## Introduction

Biodegradable nanoparticles have been developed as effective drug carriers over the past few decades. The benefits of nanoparticles in drug delivery system are (i) drug protection against in vivo degradation, (ii) stability in blood circulation, (iii) high drug encapsulation efficiency, and (iv) ability to control the drug release rate. Nanoparticles based on biodegradable PCL are being extensively investigated using poly(ethylene glycol), PEG, as a counter copolymer (PCL-PEG) to prevent recognition by reticuloendothelial system (RES). The PCL-PEG system has been used to encapsulate small drug molecules,<sup>1,2</sup> proteins,<sup>3</sup> peptides,<sup>1,4</sup> and nucleic acids.<sup>5</sup> The surface morphology and cellular uptake<sup>6</sup> have been studied by varying the molar ratios between hydrophobic PCL and hydrophilic PEG. On the other hand, the development of carriers coated with polysaccharides has also progressed in parallel to that of PEG-coated nanoparticles, not only to prevent the recognition by RES but also to target a specific receptor in certain cells or tissues.<sup>7–11</sup> PCL and dextran (PCL-DEX) nanoparticles have been synthesized and studied for their stability and interactions with biological systems.<sup>7,11–13</sup> A peer-reviewed article has well-directed us in preparations, characterizations, and applications of polysaccharide-decorated nanoparticles.<sup>13</sup> Tetriconic-PCL-heparin (and its polymeric micelles) has been prepared as an injection vehicle based on the binding character between heparin and basic fibroblast growth factor for long-term delivery.<sup>14</sup>

CS is an important structural component in connective tissues and cartilage, which has many promising properties such as biocompatibility, biodegradability, anti-inflammatory, and a good structure/disease-modifying antiosteoarthritis drug (S/DMOAD).<sup>15</sup> It appears worthwhile to use PCL as a core

decorated by CS as a shell. Because CS is a highly water soluble anionic polysaccharide, we hypothesized that the higher hydrophilic character of CS than DEX or PEG would lead to a better segregation between PCL and CS compartments and result in a lower CMC value. The low CMC value benefits the stabilization of nanoparticles circulation in a physiological condition. The other merit of CS is it belongs to one of the glycosaminoglycans that binds endogenous proteins with different functional properties, such as growth factors, adhesion molecules, or enzymes, which regulate the human immune system.<sup>16</sup> The negative charges of CS on the surface also prevent the micelle aggregation.

Instead of using the conjugation between the hydroxyl groups of sugars to the carboxylic groups of PCL commonly reported in the literature,<sup>7,17,18</sup> we introduced the vinyl groups on CS to extend its applications. The vinyl groups on CS could be used to process a free radical reaction either with the double bond end-capped PCL to form a graft copolymer or with vinyl groups on CS themselves, to form a shell cross-linked micelle. The carboxylic groups on CS were saved to react with a functional molecule that can specifically target cancer cells for our future study.

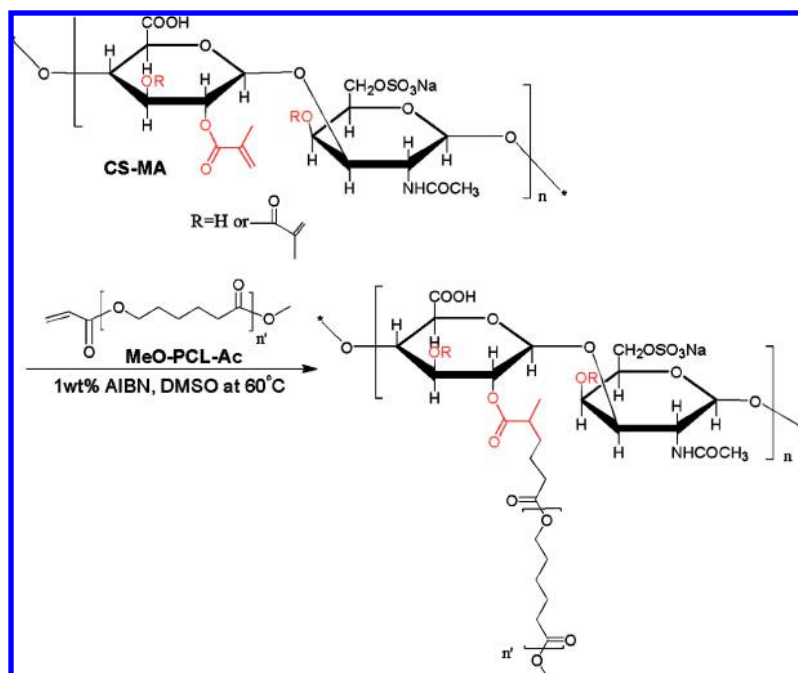
## Experimental Section

**Materials.** Sodium CS was purchased from Tohoku Miyagi Pharmaceutical Co., Ltd. (Tokyo, Japan). Its number-averaged molecular weight was 85000 g/mol, equivalent to dextran standards, as determined by GPC. Methacrylic anhydride, methanol, and acryloyl chloride were purchased from Lancaster (Lancashire, U.K.) and used as received. FITC-BSA and tris(hydroxymethyl) aminomethane were obtained from Sigma (St. Louis, MO). Fetal bovine serum (FBS) was purchased from Biological Industries (Beit Haemek, Israel). Potassium dihydrogen phosphate, disodium hydrogen phosphate, glycine, boric acid, and hydrochloric acid were obtained from Fluka (Buchs, Switzerland) and used for buffer preparation. 3-(4,5-Dimethyl-thiazol-2yl)-2,5-diphenyl tetrazolium bromide (MTT) was acquired from MP Biomedicals

\* To whom correspondence should be addressed. Tel.: 011-886-7-3121101-2217. Fax: 011-886-7-3125339. E-mail: lfwang@kmu.edu.tw.

<sup>†</sup> Kaohsiung Medical University.

<sup>‡</sup> National University of Kaohsiung.

**Scheme 1.** Synthesis Route of PCL-Grafted CS Copolymers Named PCL-CS

(Eschwege, Germany). Pyrene and  $\epsilon$ -caprolactone were purchased from Acros (New Jersey).

**Synthesis of Methacrylated Chondroitin Sulfate (CS-MA).**<sup>19</sup> CS-MA was synthesized by the procedure described in our previous publication.<sup>19</sup> The degree of substitution of methacrylate groups onto CS was controlled at 70%. The reaction solution was alcohol-precipitated, and the precipitate was filtered and washed with alcohol until no methacrylic anhydride residue was detected by NMR. The resulting CS-MA product was dried in a vacuum oven at room temperature for 24 h with a yield of  $\sim$ 90%. Two distinctive peaks at 5.65 and 6.10 ppm, which appear in the  $^1\text{H}$  NMR ( $\text{D}_2\text{O}$ ) spectrum, were attributed to the two protons attached to the double bond ( $\text{C}=\text{CH}_2$ ) and the peak shown at 1.75 ppm, ascribed to methyl groups adjacent to double bond ( $\text{CH}_3-\text{C}=\text{CH}_2$ ), which are not present in the nascent CS.

**Synthesis of Poly( $\epsilon$ -caprolactone) End-Capped with Acrylated Group (MeO-PCL-Ac).** PCL with methoxy-end groups (MeO-PCL-OH) was synthesized by mixing  $\epsilon$ -caprolactone (22.5 g, 0.197 mol) and 0.5 g (0.015 mol) of anhydrous methanol in a fire-dried polymerization tube in the presence of a dried magnetic stirring bar. The tube was connected to a vacuum line, where exhausting and refilling with Ar gas was repeated three times. The tube was closed and immersed into an oil bath preheated at 230  $^\circ\text{C}$  under Ar atmosphere for 7 h. The reaction was cooled to room temperature and 10 mL of methylene chloride was used to dissolve the product followed by precipitation into 50-fold excess of methanol. The obtained polymers were purified by successive precipitations four times using methylene chloride as a solvent and methanol as a nonsolvent. The final product was dried under vacuum with  $\sim$ 95% yield and  $^1\text{H}$  NMR ( $\text{CDCl}_3$ ,  $\delta$ , ppm) peaks for MeO-PCL-OH are 4.07 (t, 6.6 Hz, terminal  $-\text{CH}_2-\text{OCO}-$ ), 3.65 (s,  $-\text{OCH}_3$ ), 2.25 (m,  $-\text{OCO}-\text{CH}_2-\text{CH}_2-\text{CH}_2-$ ), 1.66 (m,  $-\text{OCO}-\text{CH}_2-\text{CH}_2-\text{CH}_2-\text{CH}_2-$ ), 1.39 (m,  $-\text{OCO}-\text{CH}_2-\text{CH}_2-\text{CH}_2-$ ).

A total of 5 g ( $\sim$ 2.4 mmol) of the resulting MeO-PCL-OH was dissolved in 20 mL of methylene chloride containing 1 mL of triethylamine. Acryloyl chloride (14.3 mmol) was dropwise added into the above solution within 30 min at 0  $^\circ\text{C}$ . After that, the reaction temperature was raised to room temperature and the reaction was further continued for 24 h. Then the reaction mixture was precipitated into 50-fold excess of hexane and the precipitated product was dissolved into 50 mL of methylene chloride again and extracted 4 times with doubled deionized (DI) water to remove amine salt. The product was

recovered after solvent removal by rotavapor and dried under vacuum at room temperature for 24 h. The resulting MeO-PCL-Ac is  $\sim$ 80% yield. Besides the characteristic peaks assigned for MeO-PCL-OH above,  $^1\text{H}$  NMR ( $\text{CDCl}_3$ ,  $\delta$ , ppm) spectrum for MeO-PCL-Ac appears three additional peaks at 6.35 (dd, 1.8 and 17.2 Hz, *cis*- $\text{H}_2\text{C}=\text{CH}$ ), 6.05 (dd, 10.2 and 17.2 Hz,  $\text{H}_2\text{C}=\text{CH}$ ), 5.85 (dd, 1.8 and 10.2 Hz, *trans*- $\text{H}_2\text{C}=\text{CH}$ ).

**Synthesis of PCL-CS Copolymers.** In all preparations, the MeO-PCL-Ac concentration was fixed at 2 mg/mL in dimethylsulfoxide (DMSO). A copolymer of the weight ratio between CS-MA and MeO-PCL-Ac at 1:1 is taken as an example (abbreviated as PCL-0.27 in the text). MeO-PCL-Ac (100 mg, 48  $\mu\text{mol}$ ) was completely dissolved into 50 mL of DMSO at 65  $^\circ\text{C}$  and then slowly added into CS-MA (100 mg, 189  $\mu\text{mol}$  repeating units) in 1 mL of DI water, where exhausting and refilling process was repeated in Ar atmosphere for 3 times. A total of 1 wt % 2,2'-azobisisobutyronitrile (AIBN) in DMSO relative to total weight of MeO-PCL-Ac and CS-MA was added into the reaction mixture, which was continuously stirred for 4 h at 65  $^\circ\text{C}$ . After cooling to room temperature, the reaction mixture was poured into a dialysis membrane (MWCO 6000–8000, Spectra/Pro 7, Spectrum Laboratories Inc., U.S.A.) and dialyzed against DI water, which is changed every 3–6 h for 2 days to remove DMSO and other initiator residues. The aqueous solution in dialysis tube was removed and extracted three times with methylene chloride to remove PCL residues. The aqueous solution was freeze-dried and the resulting product was stored at  $-20$   $^\circ\text{C}$  for further use. Solubility of copolymers was tested by adding 5 mg of samples into 2 mL of solvents for 30 min and observed by naked eyes. The tested solvents include DI water, acetone, chloroform, dimethylformamide (DMF), DMSO at room temperature and 60  $^\circ\text{C}$ , ethyl acetate (EA), and tetrahydrofuran (THF).

**Micelles Preparation with or without FITC-BSA.**<sup>11</sup> A total of 1 mg of PCL-CS copolymers was dispersed in 1 mL of methylene chloride and dropwise added into 10 mL of DI water with or without salt contents. The oil-in-water solution was stirred at a rate of 500 rpm for 30 min at room temperature. This emulsion was mixed under high vortex for 60 s and then methylene chloride was removed with the use of a rotavapor. The final volume was adjusted to 10 mL again. The particle size was measured at this concentration of 0.1 mg/mL.

In the other experiment, 10 mg micelles containing 1 mg FITC-BSA in the aqueous phase was scaled up and prepared as stated above. The concentration of FITC-BSA in the supernatant was determined

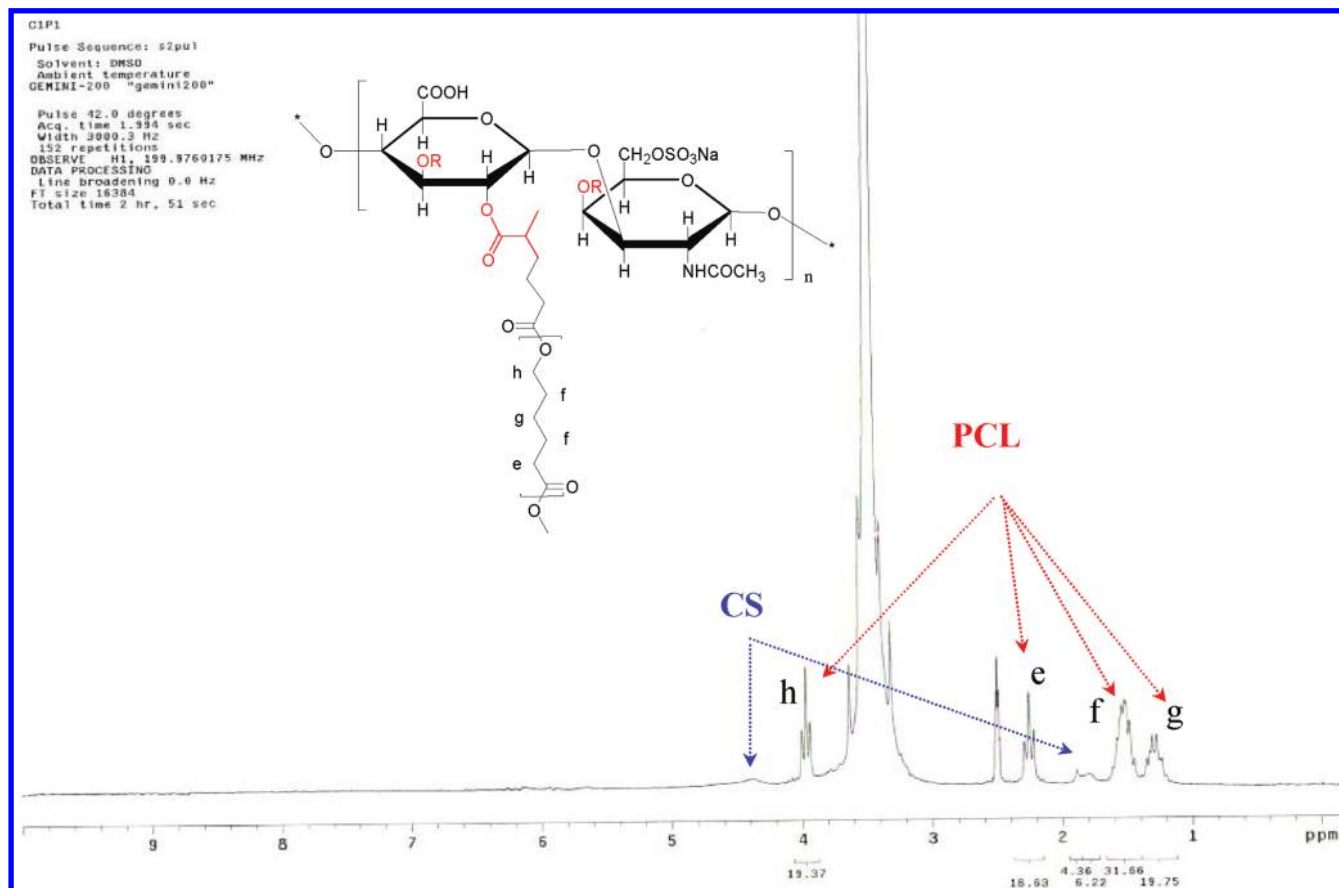


Figure 1.  $^1\text{H}$  NMR spectrum of PCL-0.27 in  $\text{DMSO-}d_6$ .

relative to a calibration curve. The supernatant solutions were separated from the precipitated micelles by centrifugation at 15000 rpm for 5 min. The drug loading and encapsulation efficiencies were calculated base on the following equations

$$\text{encapsulation efficiency} : \frac{w_0 - w_b}{w_0} \times 100\% \quad (1)$$

$$\text{loading efficiency} : \frac{w_0 - w_b}{w_c} \times 100\% \quad (2)$$

where  $w_0$ ,  $w_b$ , and  $w_c$  are FITC-BSA amount in feed and in the supernatant, and the weight of the micelles, respectively. The calibration curve of FITC-BSA was made from the various dilutions of stock solution ( $25 \mu\text{g/mL}$  in PBS at  $\text{pH} = 7.4$ ). Fluorescence spectra were recorded on a Cary Eclipse fluorescence spectrophotometer (Varian, CA) with an excitation wavelength of 495 nm and an emission wavelength of 520 nm.

**Characterizations.** FTIR spectra were obtained on a Perkin-Elmer-2000 spectrometer. Dried samples were pressed with potassium bromide (KBr) powder into pellets. A total of 64 scans were signal-averaged in the range from 4000 to  $400 \text{ cm}^{-1}$  at a resolution of  $4 \text{ cm}^{-1}$ .  $^1\text{H}$  NMR spectra were recorded on a Gemini-200 spectrometer (Varian, CA) using deuterium chloroform ( $\text{CDCl}_3$ ),  $\text{D}_2\text{O}$ , and  $\text{DMSO-}d_6$  as solvents. The melting temperature and enthalpy of PCL-CS copolymers were determined with the use of a Perkin-Elmer differential scanning calorimeter (DSC-7). Specimens were dried overnight before measurements. The scanning temperature is from  $-60$  to  $100 \text{ }^\circ\text{C}$  at the heating rate of  $10 \text{ }^\circ\text{C/min}$  under nitrogen. After the first run, the specimens were kept in sample holder at  $25 \text{ }^\circ\text{C}$  for 24 h. Then, the samples were rerun and referred as the second run in the text. The molecular weights of copolymers were measured by gel permeation chromatography (GPC), which composed of a Water Model 501 pump, a HP 1047 refractive index detector, a Shodex sugar KS-G column, and a KS-804

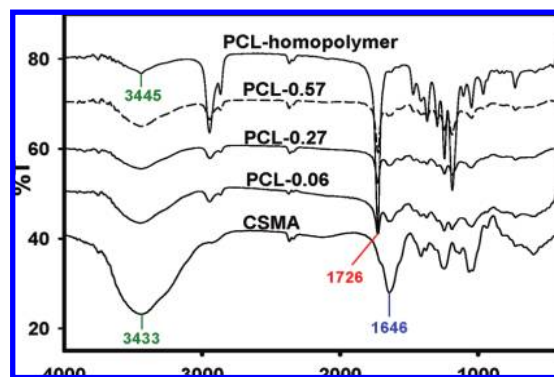


Figure 2. FTIR spectra of PCL, CS-MA, and PCL-CS copolymers.

column. DMSO was used as a mobile phase at the flow rate of  $1 \text{ mL/min}$  at  $50 \text{ }^\circ\text{C}$ . The column setting was calibrated using six monodisperse dextran standards.

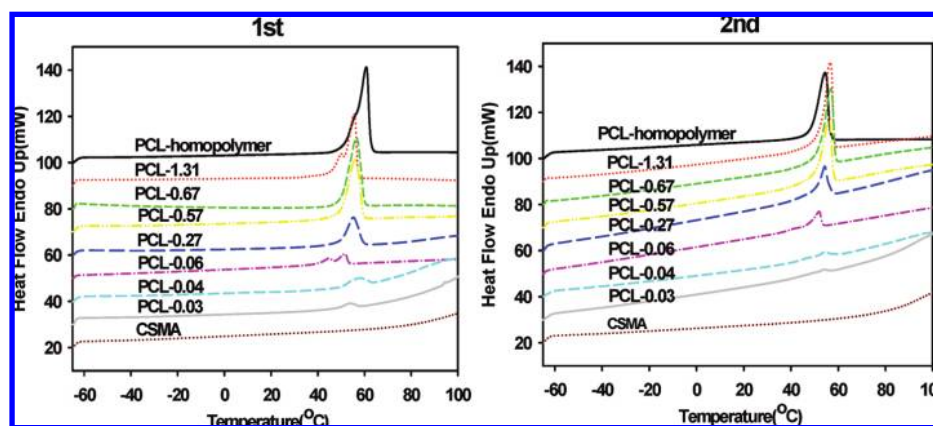
Fluorescence spectra were recorded on a Cary Eclipse fluorescence spectrophotometer. Pyrene was used as a fluorescence probe by dissolution in acetone at a concentration of  $3.08 \times 10^{-5} \text{ M}$ . A total of  $20 \mu\text{L}$  of pyrene stock solution was added into 20 individual vials, and acetone was allowed to evaporate. Each  $1 \text{ mL}$  of aqueous PCL-CS solution at different concentrations was added into vials and heated for 3 h at  $60 \text{ }^\circ\text{C}$  to equilibrate the pyrene (final concentration  $6.16 \times 10^{-7} \text{ M}$ ) and then cooled overnight in dark. Pyrene excitation spectra were recorded using an emission wavelength at 390 nm. The emission and excitation slit widths were set 2.5 and 2.5 nm, respectively. A CMC value was determined from the ratios of pyrene intensities at 339 and 336 nm and calculated from the intersection of two tangent plots of  $I_{339}/I_{336}$  versus log concentrations of polymers.<sup>20</sup>

Particle sizes of micelles were measured using a Zetasizer 3000HS dynamic light scattering (Malvern, Worcestershire, U.K.). The particles

**Table 1.** PCL Molar Fractions in Copolymers

sample codes	PCL molar fraction		PCL numbers per CS-MA repeating unit	$M_{n,GPC}^b$	$M_w/M_n^b$
	in feed	in experiment <sup>a</sup>			
PCL-1.31	0.725	0.568	1.315	68700	2.56
PCL-0.67	0.569	0.401	0.669	67100	2.70
PCL-0.57	0.442	0.363	0.570	70100	2.35
PCL-0.27	0.209	0.212	0.269	71900	2.30
PCL-0.06	0.081	0.060	0.064	61900	2.87
PCL-0.04	0.050	0.040	0.042	87500	2.00
PCL-0.03	0.026	0.027	0.028	89500	2.12

<sup>a</sup> Calcd from FT-IR measurements with a use of a calibration curve made by the known compositions of CS-MA (molecular weight of a repeating unit taken as 528 g/mol) and PCL (the number-averaged molecular weight taken as 2000 g/mol). The ratio of absorbance intensity at 1726 and 1646  $\text{cm}^{-1}$  was used to calculate PCL molar fraction. <sup>b</sup>  $M_{n,GPC}$  and  $M_w/M_n$  were determined by GPC with a use of dextran standards. DMSO was used as eluent at 50 °C.

**Figure 3.** DSC thermograms of the first heating and the second heating runs of PCL and PCL-CS copolymers.**Table 2.** Melting Temperatures, Enthalpies, and CMC Values of Copolymers

sample codes	first run			second run			recovery <sup>a</sup> (%)	CMC (mg/mL)
	onset (°C)	peak (°C)	delta H (J/g)	onset (°C)	peak (°C)	delta H (J/g)		
PCL	55.0	60.7	114.75	48.4	54.4	91.86	80.05	
PCL-1.31	50.8	55.5	90.40	53.0	56.5	96.61	106.86	$1.26 \times 10^{-3}$
PCL-0.67	50.4	56.5	92.67	52.1	56.8	82.36	89.37	$2.50 \times 10^{-3}$
PCL-0.57	50.1	55.8	78.47	51.2	56.0	70.37	89.68	$3.43 \times 10^{-3}$
PCL-0.27	49.7	55.2	42.33	50.4	54.3	30.88	72.96	$3.17 \times 10^{-3}$
PCL-0.06	46.4	51.5	19.31	46.7	51.8	20.79	107.65	$3.63 \times 10^{-3}$
PCL-0.04	50.6	57.5	10.16	49.9	54.4	8.96	88.22	$7.12 \times 10^{-3}$
PCL-0.03	48.9	53.7	4.36	49.9	53.8	3.74	85.81	$8.86 \times 10^{-3}$

<sup>a</sup> Recovery: the percentage of delta H of the second run to that of the first run.

were filtered with 0.45  $\mu\text{m}$  disk filter and measured in DI water with or without salt contents. The concentration of the sample was 0.1 mg/mL and temperature was maintained at 37 °C. CONTIN algorithms were used in the Laplace inversion of the autocorrelation function to obtain size distribution of PEC particles.<sup>21</sup> The mean diameter was evaluated from the Stokes–Einstein equation.<sup>21</sup> The particle size and morphology of the micelles were also visualized using TEM (JEM-2000 EXII, JEOL, Japan). A carbon-coated 200 mesh copper specimen grid (Agar Scientific Ltd, Essex, U.K.) was glow-discharged for 1.5 min. A total of 1 drop of the micelles was deposited on the grid and left to stand for 2 min after which time any excess fluid was removed with a filter paper. The grids were allowed to dry for 2 days at room temperature and then examined with the electron microscope.

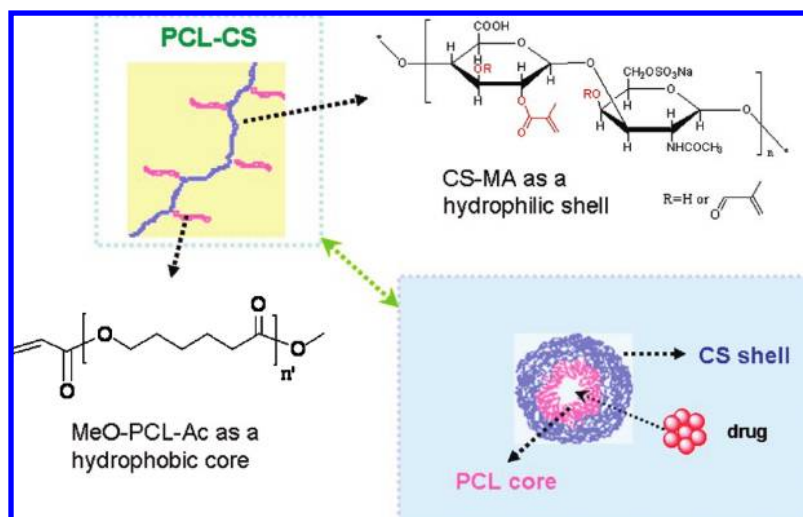
X-ray photoelectron spectroscopy (XPS) measurements were performed on a Fisons VG ESCA 210 spectrometer using a monochromated Al K $\alpha$  X-ray source. The relative atomic concentration of each element at the sample surface was calculated from the peak area using the atomic sensitivity factor specified by the manufacturer. Spectra were recorded over a range of binding energies from 0 to 1200 eV, with a pass energy of 100 eV for the wide scan survey and a pass energy of 20 eV for high energy resolution spectra for regions of C1s, N1s, O2s, and S2p.

**In Vitro Cellular Uptake of Micelles.** KB cells, an oral epidermoid cell, obtained from Dr. Cheng's group at Kaohsiung Medical University of Taiwan, were grown and maintained in RPMI 1640 medium. Each cell culture medium was supplemented with 10% inactivated fetal bovine serum (FBS), 100  $\mu\text{g/mL}$  streptomycin, and 100 U/mL penicillin at 37 °C under 5% CO<sub>2</sub>. KB cells ( $1 \times 10^5$  cells in 1 mL) were, respectively, seeded into a 12-well culture plate containing one glass coverslip/well and incubated for 24 h. After that, the medium was removed and 1 mL of free FITC-BSA- or FITC-BSA-loaded micelles in PBS (pH 7.4 and 0.2% FBS) at a concentration of 0.1 mg/mL was added into each well and incubated for 30 min at 37 °C. After incubation, coverslips were taken, washed with 2 mL of PBS three times, placed in empty wells, and treated with 1 mL of 3.7% formaldehyde in PBS for 15 min. After three additional PBS washings, the cells on the coverslips were mounted on glass slides by fluorescent mounting medium. Coverslips were sealed with a nail-polished oil and maintained at 4 °C in the dark overnight and analyzed by an Olympus FV 500 (Tokyo, Japan).

**Cytotoxicity.** KB cells were seeded in 96-well tissue culture plates at a density of  $1.5 \times 10^4$  cells per well in RPMI 1640 medium containing 10% FBS. The cytotoxicity was evaluated by determining the viability of the macrophages after incubation with different



**Scheme 2.** New Type of Core-Shell Micelles Based On Biocompatible and Biodegradable Amphiphilic Copolymers Using Chondroitin Sulfate (CS) as a Hydrophilic Segment and Poly( $\epsilon$ -caprolactone) (PCL) as a Hydrophobic Segment



concentrations of PCL-CS (10–1000  $\mu\text{g}/\text{mL}$ ) for 24 h. The number of viable cells was determined by the estimation of their mitochondrial reductase activity using the tetrazolium-based colorimetric method (MTT conversion test).<sup>22</sup> At the end of the incubation period, cells were incubated with 50  $\mu\text{L}$  of a MTT solution at a concentration of 2 mg/mL for 3 h at 37  $^{\circ}\text{C}$ . One hundred  $\mu\text{L}$  DMSO were then added in order to dissolve the formazan crystals. The UV absorbance of the solubilized formazan crystals was measured spectrophotometrically at 595 nm to determine the number of living cells. Cell viability was expressed as the amount ratio of formazan determined between the cells treated with the different concentrations of PCL-CS and the nontreated cells.

**Statistical Methods.** Means, SD, and SE of the data were calculated. Differences between the experimental groups and the control groups were tested using Student's-Newman-Keuls' test and  $P < 0.05$  were considered significant.

## Results and Discussion

**Preparation of Initial Macromers and Copolymers.** The ring opening polymerization of  $\epsilon$ -caprolactone (CL) was initiated by anhydrous methanol without using any catalysts at a high temperature of 230  $^{\circ}\text{C}$ . The peak intensity ratio shown at 3.65 ppm ( $-\text{OCH}_3$ ) to 4.07 ppm ( $-\text{CH}_2-\text{OCO}-$ ) was used to calculate the molecular weight of MeO-PCL-OH, that is,  $\sim 2000$  g/mol (Supporting Information, S1). Then, the hydroxyl groups of MeO-PCL-OH were acrylated by a reaction with a large excess of acryloyl chloride. In order to remove the large excess acryloyl chloride, the reaction mixture was precipitated in 50-fold excess of hexane, a good solvent for acryloyl chloride but a nonsolvent for PCL. Then, the precipitate was dissolved in methylene chloride and extracted with DI water to remove the triethylamine salt. MeO-PCL-Ac was confirmed by  $^1\text{H}$  NMR (Supporting Information, S2). The characteristic peaks appearing at 5.85, 6.06, and 6.35 ppm are the evidence of three protons attached on C=C double bonds. The averaged peak intensity of three protons to those of the methoxy groups at 3.65 ppm was used to calculate the degree of acrylation for MeO-PCL-Ac, that are in the range of 90.4 to 93.3% from different synthesis batches. CS-MA was synthesized followed the method reported previously.<sup>19</sup> The peak intensity at 1.75 ppm to that at 1.86 ppm, corresponding to the methyl groups on double bonds and the acetyl groups of nascent CS, was used to calculate the degree of MA reacting with hydroxyl groups of CS, that is,  $\sim 70\%$  per repeating unit (Supporting Information, S3).

We chose the high degree of MA substitution on CS-MA for two reasons. First, the solubility problem exists between PCL (dissolves in organic solvents) and CS (dissolves in water only). The solubility of CS-MA in DMSO increases with an increase in degrees of MA substitution,<sup>19</sup> and a homogeneous condition is more beneficial than a heterogeneous condition to

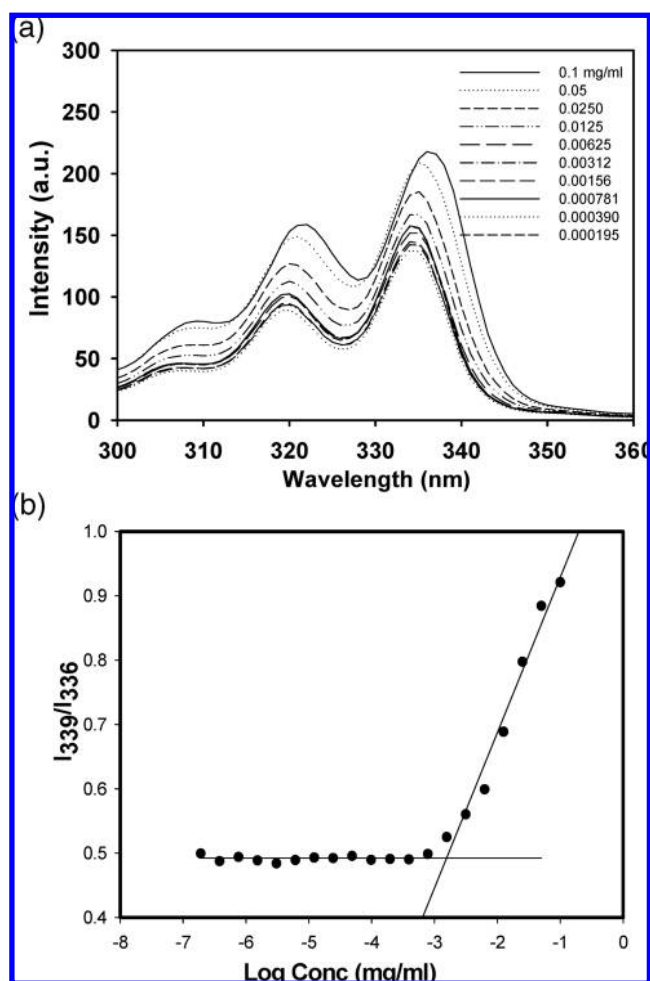


**Figure 4.** Excitation spectra of pyrene in PCL-0.27 at a fixed emission wavelength of 390 nm in various concentrations (a) and a plot of  $I_{339}/I_{336}$  vs log concentrations to determine the critical micelle concentration (b).

obtain a successful graft copolymerization. Second, the higher the degree of MA substitution, the higher the possibility double bonds can be saved on a shell compartment for the future application. CS-MA with 70% MA substitution could be dissolved in DMSO at 65 °C. Thus, the various molar ratios between CS-MA and MeO-PCL-Ac in feed were synthesized at a concentration of 2 mg/mL in DMSO at 65 °C; the reaction equation is depicted in Scheme 1. A typical  $^1\text{H}$  NMR spectrum of PCL-0.27 with assignments is shown in Figure 1. The major resonance peaks indicated as e–h were attributed to PCL. The sugar methylene proton signals  $\sim 4.4$  ppm and two distinguishable peaks centered at 1.75 and 1.86 ppm were, respectively, attributed to methyl groups attached on double bonds and N-acetyl groups of CS-MA. This result indicates the successfully grafting reaction between CS-MA and MeO-PCL-Ac. The peak at 1.75 ppm becomes broad in PCL-0.27 in comparison to that of CS-MA, and implies that there are still some residual double bonds left on CS-MA. These remaining double bonds can be saved for crossing the shell compartment or forming a reaction with functional molecules in a future study. Though the NMR is a good technique to calculate the molar ratio between two component polymers, however, the CS signals of copolymers with a high composition of PCL become ambiguous. Thus, the copolymer compositions were determined from FT-IR spectra (Figure 2). The -OH and -NH stretching in the 3000–3500  $\text{cm}^{-1}$  region and the maximum signal of -CONH amide at 1646  $\text{cm}^{-1}$  were mainly attributed to CS. The aliphatic C–H stretching appearing at 2900  $\text{cm}^{-1}$  and carbonyl -COO absorbance at 1726  $\text{cm}^{-1}$  were due to PCL. A calibration curve based on the intensity ratios between 1726 and 1646  $\text{cm}^{-1}$  vs the known molar ratios between PCL homopolymer and CS-MA repeating unit was carried out. The molar fraction of PCL in each PCL-CS copolymer was calculated and represented as a numeral after PCL in Table 1. The experimental fractions of PCL in the copolymers show a good linear correlation with those in feed. The solubility test of the graft copolymers in several solvents shows that PCL-CS copolymers did not dissolve in DI water, acetone, chloroform, DMF, DMSO, EA, and THF at room temperature, but slightly dissolved in DMSO at 60 °C. Because of a solubility problem, the number-average molecular weights of these copolymers measured by GPC show a broad polydispersities ( $M_w/M_n$ ) in the range of 2.00–2.87, as listed in Table 1.

The thermal behaviors of copolymers were analyzed by DSC.<sup>23</sup> Because the melting temperature of CS supplied by manufacture (204 °C) is close to its degradation temperature, the endothermic peaks attributed to PCL crystalline domains were only traced. Figure 3 shows DSC thermograms of copolymers in their first (Figure 3a) and second (Figure 3b) heating runs, indicating a single melting peak at  $\sim 60$  °C. The melting point depression of PCL segments was clearly seen in the first run and decreased with an increasing amount of CS in copolymers. The presence of CS in copolymers hinders the crystallization of PCL segments. The melting peak of PCL is 60 °C in the first run and drops to 54 °C in the second run. However, for copolymers, the melting temperatures attributed to PCL do not show a significant change between the first and the second runs. If we define the crystallinity recovery as the enthalpy ratios between the second and the first runs, we find that the recovery of crystallized PCL segments (except PCL-0.27) and the melting temperatures (except PCL-0.06) are higher in copolymers than PCL homopolymer itself as tabulated in Table 2. The decrease in the PCL crystallinity in the second run is less severe in copolymers than its homopolymer, implying

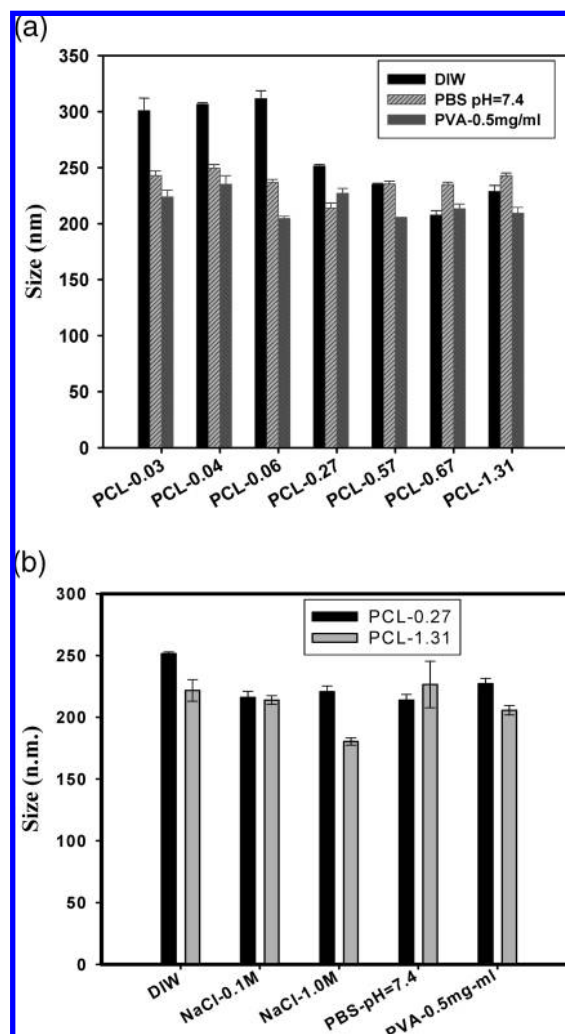


**Figure 5.** Average hydrodynamic sizes of PCL-CS micelles at a concentration of 0.1 mg/mL in double deionized water (DIW), 0.1 M phosphate buffer solution at pH 7.4, and DIW with 0.5 mg/mL polyvinyl alcohol (a); average hydrodynamic sizes of PCL-0.27 and PCL-1.31 in various medium solutions (b).

the better self-assembled ability of PCL into crystalline domains when a hydrophilic CS counterpart is present. This phenomenon is analogous to that of the H-bonding formation among the carboxylic groups of poly(acrylic acid) which is enforced when the hydrophobic styrene was copolymerized.<sup>24</sup> Similarly, the presence of hydrophilic CS segments enhance the crystallization rate of PCL segments.

**Critical Micelle Concentrations (CMC).**<sup>20</sup> As copolymers were synthesized, they were assembled through a simple emulsion-solvent evaporation method to form micelles in an aqueous solution due to the segregation between the hydrophobic and hydrophilic segments as illustrated in Scheme 2. CMC was determined using pyrene as a fluorescent probe as a typical example shown in Figure 4a for PCL-0.27. Because of the hydrophobic character of pyrene, once the micelles were formed in an aqueous solution, pyrene molecules were incorporated into the hydrophobic core of the micelles. The transfer of pyrene from the polar environment to a nonpolar region significantly increased the intensity ratio of  $I_{339}/I_{336}$ . Thus, the concentration that dramatically increases in the plot of  $I_{339}/I_{336}$  versus copolymer concentrations was recorded as CMC as illustrated in Figure 4b. The CMC values of PCL-CS with the various compositions between CS and PCL are tabulated in Table 2. Though there are many factors that affect the CMC values of

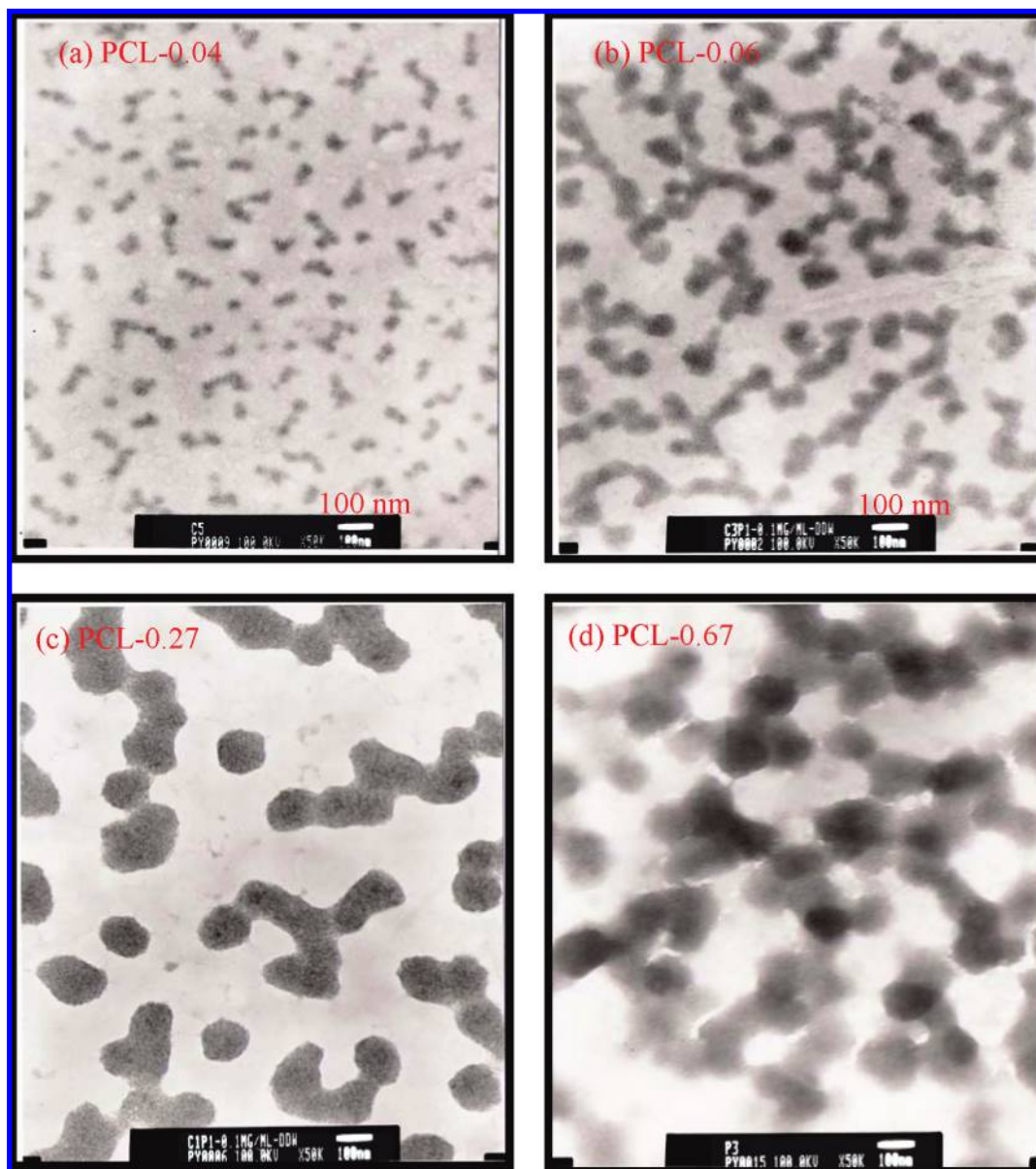


**Figure 6.** TEM images of PCL-CS micelles at a concentration of 0.1 mg/mL in double deionized water: PCL-0.04 (a), PCL-0.06 (b), PCL-0.27 (c), and PCL-0.67 (d).

block copolymer micelles, the most profound impact on CMC values is the hydrophobicity of core-forming block. The increase in hydrophobicity lowered the CMC value.<sup>25</sup> The CMC value of  $8.86 \times 10^{-3}$  mg/mL for PCL-0.03 decreases to that of  $1.26 \times 10^{-3}$  mg/mL for PCL-1.31. The increase in the molar fractions of PCL of the copolymers slightly lowers the CMC values in PCL-CS. As compared CMC values of PCL-CS with those of MePEG-*b*-PCL, we find that MePEG-*b*-PCL shows an inverse correlation between CMC values and the lengths of PCL block significantly.<sup>26</sup> The CMC values of MePEG-*b*-PCL are in the range from  $6.97 \times 10^{-1}$  to  $3.38 \times 10^{-3}$  mg/mL as the PCL block length increased from 2 to 10.<sup>27</sup> In PCL-CS, the molecular weight of PCL is  $\sim 2000$  g/mol and the numbers of the PCL repeating unit are fixed at  $\sim 18$ . This PCL length is long enough for self-assembly between CS and PCL. Changing the molar ratios between CS-MA and PCL in feed may only affect on the degree of PCL grafted onto CS-MA but not on the CMC values. The CMC values are comparative lower in PCL-CS than in MePEG-*b*-PCL, implying the lower disassocia-

tion of micelle into unimers if diluted in the biological environment.

**Micelle Sizes and Stability.** The average hydrodynamic sizes of PCL-CS were tested in DI water, 0.1 M phosphate-buffered saline at pH 7.4 (PBS), and DI water with the presence of 0.5 mg/mL polyvinyl alcohol (PVA), as shown in Figure 5a. In pure DI water, the particle sizes of PCL-0.03, PCL-0.04, and PCL-0.06 are  $\sim 300$  nm and the rest of the copolymers have the smaller hydrodynamic sizes ranging from 208 to 250 nm. The hydrodynamic sizes of micelles tested in PBS or DI water with the PVA surfactant show relatively smaller sizes than those measured in pure DI water and the change in the hydrodynamic particle sizes is insignificant with the variation of molar fractions of PCL in the copolymers. This situation may be due to that CS is an ionic polysaccharide bearing the negative charges, which attract counter positive ions in PBS and form a shielded layer of outer surface to prevent water penetration and swelling particles. Because the swelling of the outer shell increases with an increase in CS compositions of the copolymers, PCL-0.03,



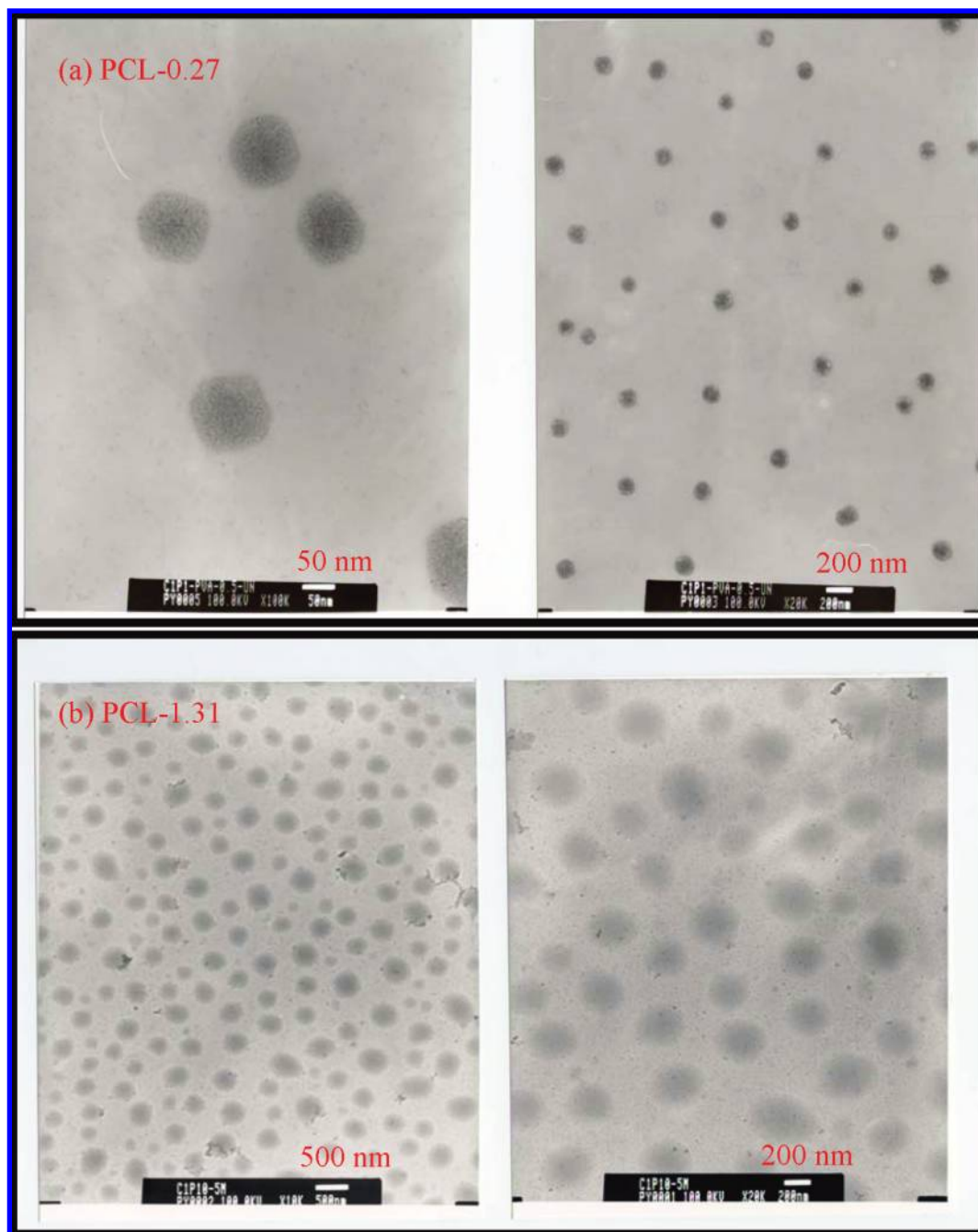


**Figure 7.** TEM images of PCL-0.27 (a) and PCL-1.31 (b) at a concentration of 0.1 mg/mL in DIW with 0.5 mg/mL polyvinyl alcohol.

PCL-0.04, and PCL-0.06, with the high compositions of CS lead to the larger hydrodynamic sizes in DI water. The swelling behavior of CS is prohibited when CS forms the electrostatic interactions with its counterions or if shielded by a surfactant such as PVA. Though the overall hydrodynamic sizes of micelles are primarily dependent on the relative proportion of hydrophilic and hydrophobic segments in the copolymers, however, surfactants or salts also impact the unimer chains packing into micelles.<sup>28</sup> As seen in Figure 5b, the average particle sizes of PCL-0.27 and PCL-1.31 are 252 and 230 nm in DI water and decrease to 216 and 214 nm in 0.1 M NaCl solution and 220 and 180 nm in 1.0 M NaCl solution. The hydrodynamic particle sizes of PCL-0.27 and PCL-1.31 tested in 0.1 M PBS at pH 7.4 and DI water with PVA are also shown in Figure 5b for comparison. The hydrodynamic particle sizes of PCL-1.31 are stable in the salt or PVA

solutions even after 15 days stored at room temperature. Compared the particle sizes prepared freshly with those stored after 15 days in the presence of PVA or salts, the size changes are within 4% but the serious aggregation of PCL-1.31 was observed in DI water after 15 days.

The morphology of the self-assembled PCL-CS prepared from DI water was investigated by TEM as shown in Figure 6. All PCL-CS micelles appear a spherical structure with aggregation. Because PVA has been widely used as a stabilizer to disperse micelles homogeneously,<sup>2</sup> the correlation of PVA concentrations on the sizes of poly(lactic acid) (PLA) nanoparticles indicated that the PLA particle sizes decreased with an increase in PVA concentrations tested.<sup>29</sup> Indeed, the better dispersed micelles were seen in PCL-0.27 and PCL-1.31 if PVA was used at a concentration of 0.5 mg/mL, as shown in Figure 7. PCL-0.27



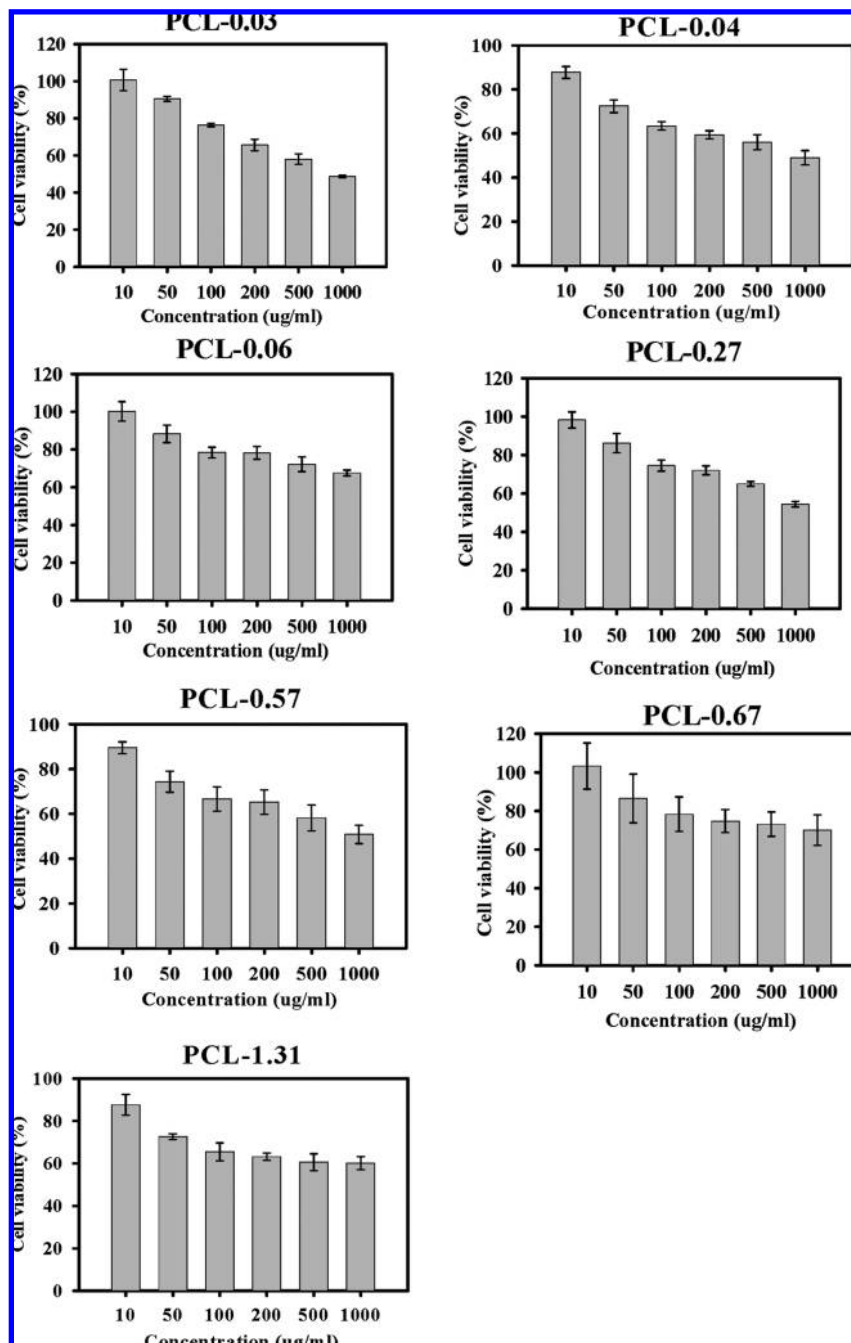


**Figure 8.** Cell viability of KB cells upon incubation with various concentrations of PCL-CS micelles for 24 h.

shows the severe size discrepancy measured by DLS and TEM (227 and 100 nm). In contrast, PCL-1.31 with the higher content of PCL segments results in similar particle sizes (206 nm by DLS and 212 nm by TEM). The fact is that the sample of TEM was carried out in a dehydrated state, but DLS was done in a solution. The copolymers containing the more hydrophilic segments result in the higher degree of swelling in micelles.<sup>30</sup> This explains why PCL-0.27 shows a severe size discrepancy between DLS and TEM measurements.

**Cytotoxicity.** Cytotoxicity studies as determined by MTT assay demonstrates that KB cells incubated with the PCL-CS micelles for 24 h remained ~100% cell viability at a concentration of 10 µg/mL. Cytotoxicity increases gradually with an increase in PCL-CS concentrations as shown in Figure 8. The cell viability remained ~60–70% even at the concentration of 1000 µg/mL of PCL-CS. CS is a natural nontoxic polymer, but

PCL has been reported to increase cytotoxicity with an increase in its concentrations.<sup>31</sup> Nevertheless, in PCL-CS, the variation of PCL compositions on cytotoxicity is trivial. This may be due to the robust self-assembly between CS and PCL, in which PCL segments are embedded inside the core and CS segments are most exposed to the outside surface. The main cause of cytotoxicity is due to the high degree of MA substitution on CS-MA used in this study. In our previous study,<sup>32</sup> the cytotoxicity study of CS-MA with the various degrees of MA substitution tested in 293T cells, mesenchymal stem cells (MSC), and human dermal fibroblast (HDF). The results showed that cell viability decreased with an increase in degrees of MA substitution onto CS and depended on the cell types pronouncedly. CS-MA with 75% MA was nontoxic to MSC but only 60% cell viable to 293T cells.

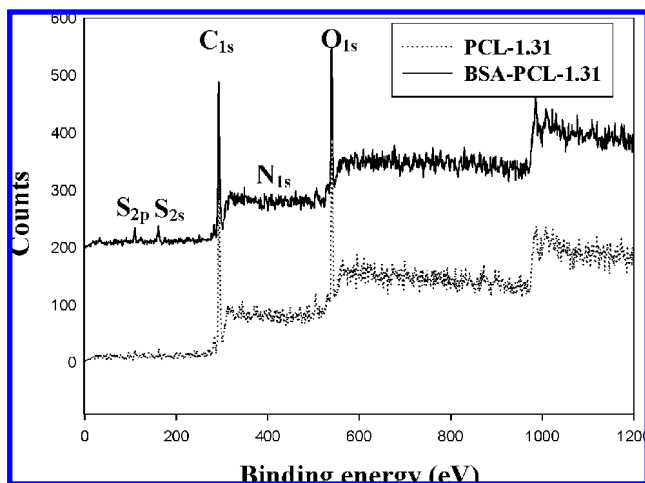


**Figure 9.** XPS spectra of PCL-1.31 and FITC-BSA-loaded PCL-1.31.

**Table 3.** Atomic Analysis of XPS of PCL

atomic	center eV	PCL-1.31	BSA-PCL-1.31
C <sub>1s</sub>	284.7	77.5%	74.2%
O <sub>1s</sub>	531.5	22.5%	24.0%
N <sub>1s</sub>	397.4	0.0	1.8%
S <sub>2p</sub>	167.5	0.0	0.0

#### Drug Loading and Intracellular Uptake in KB Cells.

FITC-BSA was used as a model protein drug to preliminarily test encapsulation efficiency of PCL-CS. Because the drug was loaded during the emulsion of micelles, the FITC-BSA deposition on micelle surface was confirmed cleanly, by tracing the FITC-BSA residue in the supernatant after three PBS washes. The drug encapsulation efficiency (EE) and loading efficiency (LE) are  $85.7\% \pm 1.8$  and  $7.8\% \pm 1.2$  for PCL-0.04;  $91.0\% \pm 0.2$  and  $8.3 \pm 0.1$  for PCL-0.67, respectively. PCL-0.67 with the PCL-rich composition shows slightly higher encapsulation efficiency for FITC-BSA. The EE values of PCL-CS are higher than those reported for PCL-Dextran, where EE values were in the range of 30–32%.<sup>12</sup> This result supports our hypothesis that the bigger difference in solubility between two counter polymers to form an amphiphilic copolymer leads to a better segregation between the core and shell compartments and the dense core will enhance the drug loading capacity.

In parallel, we also used XPS to confirm the encapsulation of FITC-BSA into PCL-CS micelles. PCL-1.31 with the lowest content of CS and highest content of PCL was chosen as an example because the drug encapsulation efficiency increased with an increase in the composition of hydrophobic core in amphiphilic copolymers.<sup>33</sup> The percentage composi-

tions obtained from the XPS analysis are atom percentage values as indicated in Figure 9 and summarized in Table 3. Though PCL-CS has nitrogen atoms, however, the atom percentage of nitrogen (N) is undetectable in PCL-1.31. The N percentage of the FITC-BSA loaded PCL-1.31 differs substantially from the values for PCL-1.31. The theoretical N percentage in PCL-1.31 is 0.45% but undetectable in the XPS analysis. Nevertheless, BSA-PCL-1.31 shows 1.8% N percentage. Moreover, the S percentages in PCL-1.31 and BSA-PCL-1.31 are untraceable but the better binding energy signal at 166.2 eV attributed to S<sub>2p</sub> is clearly seen in the latter. These XPS results indeed explain that BSA molecules were encapsulated inside PCL-CS.

The confocal microscopic technique was used to evaluate the intracellular uptake of FITC-BSA loaded with PCL-0.04 and PCL-0.67. When KB cells reached a confluency of 70–80%, they were incubated with FITC-BSA loaded micelles at a concentration of 100  $\mu\text{g}/\text{mL}$  for 30 min. Figure 10 shows that both PCL-0.04 and PCL-0.67 were endocytosed by KB cells as confirmed by the presence of green fluorescence in the cytoplasm, but the naked FITC-BSA was localized on the cell membrane with small amounts of cellular internalization. Comparing the fluorescent intensity of PCL-0.67 to that of PCL-0.04, PCL-0.67 with the higher composition of PCL segments shows a better intracellular uptake in KB cells.

#### Conclusions

The novel grafted copolymers based on CS and PCL are successfully synthesized through a simple free radical reaction. The molar fraction of PCL in the copolymers calculated from FTIR measurements correlates linearly with PCL compositions in feed. The melting temperatures and degree of crystallinity of PCL-CS increase with the increase in the molar fraction of PCL in the copolymers. The recrystallization rate of PCL segments can be enhanced if CS is present. The CMC value slightly decreases with an increase in the molar fraction of PCL in the copolymers and the particle sizes can be reduced with the use of salts or PVA. The particle sizes of PCL-CS ranged from 170 to 300 nm, increasing with an increase in PCL compositions. The TEM images of PCL-CS show a homogeneous dispersion of nanoparticles in the presence of PVA. Because of the high degree of MA substitution onto CS-MA used in this study, the cell viability was  $\sim 60\%$  when using a high concentration of 1 mg/mL incubated with KB cells for 1 day. FITC-BSA encapsulated with PCL-CS shows a better cellular internalization than free FITC-BSA.

**Acknowledgment.** We are grateful for the financial support from the National Science Foundation of Taiwan under Grant NSC 95-2221-E-037-006-MY3.

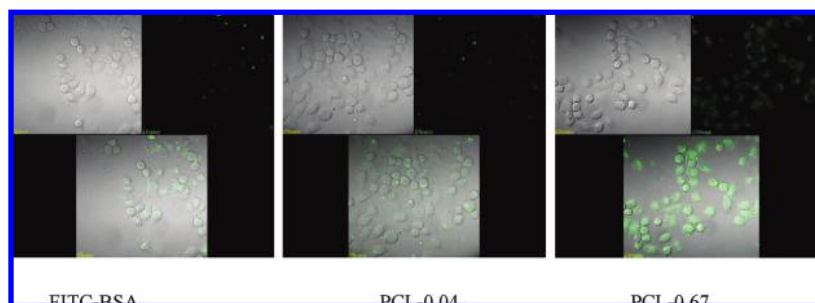


**Figure 10.** Confocal microscopic images of cellular internalization of KB cells after incubation with FITC-BSA (a), FITC-BSA-loaded PCL-0.04 (b), and FITC-BSA-loaded PCL-0.67 (c) at a concentration of 100  $\mu\text{g}/\text{mL}$  for 30 min.

## Abbreviations

AIBN: 2,2'-azobisisobutyronitrile  
 BSA: bovine serum albumin  
 CS: chondroitin sulfate  
 CS-MA: methacrylated chondroitin sulfate  
 DMSO: dimethylsulfoxide  
 FBS: fetal bovine serum  
 MTT: 3-(4,5-dimethyl-thiazol-2yl)-2,5-diphenyl tetrazolium bromide  
 MeO-PCL-OH: methoxy end-capped poly( $\epsilon$ -caprolactone)  
 MeO-PCL-Ac: methoxy end-capped poly( $\epsilon$ -caprolactone) acrylate  
 PEG: poly(ethylene glycol)  
 PCL: poly( $\epsilon$ -caprolactone)  
 PCL-CS: poly( $\epsilon$ -caprolactone) grafted chondroitin sulfate copolymers  
 FITC-BSA: fluorescein isothiocyanate labeled bovine serum albumin  
 CLSM: confocal laser scanning microscope  
 CMC: critical micelle concentrations  
 DSC: differential scanning calorimeter  
 DLS: dynamic light scattering  
 FTIR: Fourier transform infrared spectrometer  
 GPC: gel permeation chromatography  
 NMR: nuclear magnetic resonance spectrometer  
 TEM: transmission electron microscope  
 XPS: X-ray photoelectron spectroscopy

**Supporting Information Available.** NMR spectra of MeO-PCL-OH, MeO-PCL-Ac, and 70% CS-MA. This material is available free of charge via the Internet at <http://pubs.acs.org>.

## References and Notes

- Garinot, M.; Fievez, V.; Pourcelle, V.; Stoffelbach, F.; des Rieux, A.; Plapied, L.; Theate, I.; Freichels, H.; Jerome, C.; Marchand-Brynaert, J.; Schneider, Y. J.; Preat, V. *J. Controlled Release* **2007**, *120*, 195–204.
- Sonaje, K.; Italia, J. L.; Sharma, G.; Bhardwaj, V.; Tikoo, K.; Kumar, M. N. *Pharm. Res.* **2007**, *24*, 899–908.
- Liu, J.; Zeng, F.; Allen, C. *Eur. J. Pharm. Biopharm.* **2007**, *65*, 309–319.
- Pourcelle, V.; Devouge, S.; Garinot, M.; Preat, V.; Marchand-Brynaert, J. *Biomacromolecules* **2007**, *8*, 3977–3983.
- Nahar, M.; Dutta, T.; Murugesan, S.; Asthana, A.; Mishra, D.; Rajkumar, V.; Tare, M.; Saraf, S.; Jain, N. K. *Crit. Rev. Ther. Drug Carrier Syst.* **2006**, *23*, 259–318.
- Hu, Y.; Xie, J.; Tong, Y. W.; Wang, C. H. *J. Controlled Release* **2007**, *118*, 7–17.

- Lemarchand, C.; Gref, R.; Lesieur, S.; Hommel, H.; Vacher, B.; Besheer, A.; Maeder, K.; Couvreur, P. *J. Controlled Release* **2005**, *108*, 97–111.
- Bravo-Osuna, I.; Ponchel, G.; Vauthier, C. *Eur. J. Pharm. Sci.* **2007**, *30*, 143–154.
- Yu, H.; Wang, W.; Chen, X.; Deng, C.; Jing, X. *Biopolymers* **2006**, *83*, 233–242.
- Chung, T. W.; Liu, D. Z.; Hsieh, J. H.; Fan, X. C.; Yang, J. D.; Chen, J. H. *J. Nanosci. Nanotechnol.* **2006**, *6*, 2902–2911.
- Lemarchand, C.; Couvreur, P.; Besnard, M.; Costantini, D.; Gref, R. *Pharm. Res.* **2003**, *20*, 1284–1292.
- Rodrigues, J. S.; Santos-Magalhaes, N. S.; Coelho, L. C.; Couvreur, P.; Ponchel, G.; Gref, R. *J. Controlled Release* **2003**, *92*, 103–112.
- Lemarchanda, C.; Gref, A.; Couvreur, P. *Eur. J. Pharm. Biopharm.* **2004**, *58*, 327–341.
- Lee, J. S.; Go, D. H.; Bae, J. W.; Lee, S. J.; Park, K. D. *J. Controlled Release* **2007**, *117*, 204–209.
- Volpi, N. *Curr. Med. Chem.* **2005**, *4*, 221–234.
- Spillmann, D. *Biochimie* **2001**, *83*, 811–817.
- Besheer, A.; Hause, G.; Kressler, J.; Mader, K. *Biomacromolecules* **2007**, *8*, 359–367.
- Hu, F. Q.; Ren, G. F.; Yuan, H.; Du, Y. Z.; Zeng, S. *Colloids Surf., B* **2006**, *50*, 97–103.
- Wang, L. F.; Shen, S. S.; Lu, S. C. *Carbohydr. Polym.* **2003**, *52*, 389–396.
- Liu, X. M.; Pramoda, K. P.; Yang, Y. Y.; Chow, S. Y.; He, C. *Biomaterials* **2004**, *25*, 2619–2628.
- Sachl, R.; Uchman, M.; Matejicek, P.; Prochazka, K.; Stepanek, M.; Spirkova, M. *Langmuir* **2007**, *23*, 3395–3400.
- Mosmann, T. *J. Immunol. Methods* **1983**, *65*, 55–63.
- Yuan, W.; Yuan, J.; Zhang, F.; Xie, X. *Biomacromolecules* **2007**, *8*, 1101–1108.
- Wang, L. F.; Pearce, E. M.; Kwei, T. K. *J. Polym. Sci., Part C: Polym. Lett.* **1990**, *28*, 317–325.
- Astafieva, I.; Zhong, X.; Eisenberg, A. *Macromolecules* **1993**, *26*, 7339–7352.
- Letchford, K.; Liggins, R.; Burt, H. *J. Pharm. Sci.* **2008**, *97*, 1179–1190.
- Letchford, K.; Zastre, J.; Liggins, R.; Burt, H. *Colloids Surf., B* **2004**, *35*, 81–91.
- Layre, A. M.; Couvreur, P.; Richard, J.; Requier, D.; Eddine Ghermani, N.; Gref, R. *Drug Dev. Ind. Pharm.* **2006**, *32*, 839–846.
- Zambaux, M. F.; Bonneaux, F.; Gref, R.; Maincent, P.; Dellacherie, E.; Alonso, M. J.; Labrude, P.; Vigneron, C. *J. Controlled Release* **1998**, *50*, 31–40.
- Bodnar, M.; Hartmann, J. F.; Borbely, J. *Biomacromolecules* **2006**, *7*, 3030–3036.
- De Santis, R.; Catauro, M.; Di Silvio, L.; Manto, L.; Raucci, M. G.; Ambrosio, L.; Nicolais, L. *Biomaterials* **2007**, *28*, 2801–2809.
- Tsai, M. F.; Tsai, H. Y.; Peng, Y. S.; Wang, L. F.; Chen, J. S.; Lu, S. C. *J. Biomed. Mater. Res.* **2007**, *84A*, 727–739.
- Arifin, D. R.; Palmer, A. F. *Biomacromolecules* **2005**, *6*, 2172–2181.

BM800485X